Results and Status of the Cryogenic Dark Matter Search (CDMS)

R.W. Schnee [a,b,1], D.S. Akerib [a,b], P.D. Barnes Jr [c],
D.A. Bauer [d], P.L. Brink [e], B. Cabrera [e], D.O. Caldwell [d],
R.M. Clarke [e], P. Colling [e], M.B. Crisler [f], A. Da Silva [b],
A.K. Davies [e], B.L. Dougherty [e], S. Eichblatt [f], K.D. Irwin [e],
R.J. Gaitskell [b], S.R. Golwala [b], E.E. Haller [g,h], J. Jochum [b],
W.B. Knowlton [g,h], V. Kuzminov [i], S.W. Nam [e], V. Novikov [i],
M.J. Penn [e], T.A. Perera [a,b], R.R. Ross [b,g,j], B. Sadoulet [b,g,j],
T. Shutt [b], A. Smith [g], A.H. Sonnenschein [d], A.L. Spadafora [b],
W.K. Stockwell [b,j], S. Yellin [d], B.A. Young [k],

[a] *Department of Physics, Case Western Reserve University, Cleveland OH 44106*
[b] *Center for Particle Astrophysics, University of California, Berkeley CA 94720*
[c] *Lawrence Livermore National Laboratory, Livermore CA 94550*
[d] *Department of Physics, University of California, Santa Barbara CA 93106*
[e] *Department of Physics, Stanford University, Stanford CA 94305*
[f] *Fermi National Accelerator Laboratory, Batavia IL 60510*
[g] *Lawrence Berkeley National Laboratory, Berkeley CA 94720*
[h] *Department of Material Science and Mineral Engineering, University of California, Berkeley CA 94720*
[i] *Baksan Neutrino Observatory, Institute for Nuclear Research, Russian Academy of Science*
[j] *Department of Physics, University of California, Berkeley CA 94720*
[k] *Department of Physics, Santa Clara University, Santa Clara CA 95053*

Abstract

The Cryogenic Dark Matter Search experiment uses cooled germanium and silicon detectors for a direct search for weakly-interacting massive particles in our Galaxy. The novel detectors allow a high degree of background rejection by discriminating between electron and nuclear recoils through the simultaneous measurement of the energy deposited in phonons and ionization. Exposures on the order of one kilogram-day from initial runs of our experiment yield (preliminary) upper limits on the WIMP-nucleon cross section that are comparable to much longer runs of other

Preprint submitted to Elsevier Preprint *8 May 1998*

experiments. Current and future runs promise significant improvement, primarily due to improved detectors and reduced surface-electron backgrounds.

1 Introduction

Observations of stars and galaxies over a large range of distance scales indicate that most of the matter in the universe is “dark,” seen only through its gravitational effects [1,2]. Further observations imply that that much of the dark matter is non-baryonic and “cold” [3]. The Cryogenic Dark Matter Search (CDMS) experiment is an attempt to directly detect WIMPs, or weakly-interacting massive particles, a generic candidate for non-baryonic cold dark matter.

The experimental challenge is defined in part by considerations of the early Universe and the properties of our Galaxy. Constraints from the thermal production of WIMPs in the early universe that yield a dominant WIMP density today are satisfied by particles with masses in the 10–1000 GeV/c^2 range and cross sections on the scale of the weak interaction [4]. This range of particle properties suggests that supersymmetry or other extensions to the standard model may provide the dark matter [5]. If WIMPs exist they would now make up a major component of the dark matter in our own galactic halo [6]. For a standard halo comprised of WIMPs with a Maxwellian velocity distribution characterized by $v_{\mathrm{rms}} = 270$ km/s and a mass density of 0.4 GeV/cm^3, the expected rate for WIMP-nuclear scattering is in the range 1–0.001 events per kilogram of detector per day, and the expected recoil energy is as low as 1 keV [5,7].

Despite considerable worldwide efforts, WIMPs have not yet been detected. Ultimately, experiments have been dominated by irreducible backgrounds, primarily photons and electrons from radioactive contamination or activation. Further progress can be made by discriminating these background events from WIMP events. The CDMS experiment allows rejection of 99% of the photon background by using detectors that simultaneously measure the recoil energy in both phonon- and charge-mediated signals [8,9]. The ratio Y of the two measurements distinguishes electron-recoil events due to background photons from nuclear-recoil events such as those due to WIMPs, since nuclear recoils are less ionizing. Following a decade-long development effort, detectors began running in a low-background environment in 1996. Our early data runs yield preliminary upper bounds on the WIMP-nucleon cross section that are com-

---

[1] Corresponding author. E-mail: schnee@leland.stanford.edu

parable to much longer exposures of other experiments, illustrating the power of this technique.

2 Description of the Experiment

Key to the experiment is the simultaneous measurement of recoil energy ΔE in both phonon-mediated signals and ionization. The ionization measurement is made by applying a small (~ 2 V/cm) bias voltage across the two sides of the semiconductor targets. Electron-hole pairs are collected efficiently throughout the bulk of the detectors, resulting in FWHM energy resolutions as good as 640 eV. Unfortunately, trapping sites near detector surfaces result in a 10–30-μm-thick "dead layer" where charge collection is incomplete [10].

The CDMS detectors employ two distinct technologies for performing the phonon-mediated measurement of the energy deposited in a scattering event [11]. One technology uses two neutron-transmutation-doped (NTD) germanium thermistors eutectically bonded to 1.3-cm-thick 6-cm-diameter 165-g cylindrical crystal of high-purity germanium. When the device is in contact with a 20 mK bath, monitoring the thermistor resistance gives the temperature rise $\Delta T = C^{-1}\Delta E$, where C is the heat capacity. The resulting energy measurement has a FWHM resolution of 650 eV at 10 keV. The use of two NTDs permits the rejection of events that originate in an NTD and would otherwise mimic the small ionization of a nuclear recoil.

The other technology uses quasiparticle-trap-assisted electrothermal-feedback transition-edge sensors (QETs). Tungsten meanders on a surface of a cooled 1-cm-thick cylindrical detector are held in the middle of its superconducting transition by electrothermal feedback using a voltage bias. Deposited energy drives the tungsten towards normal conduction, producing a current signal. The time integral of this signal is proportional to the deposited energy, which is measured to 650 eV (FWHM) in our 100-gram silicon targets; the technology is now being transferred to germanium targets. Since the phonon collection time is fast (a few microseconds), relative-timing information from the four sensors on a device allows a two-dimensional determination of the event position to a few millimeters. Timing information also promises the ability to reject events on the top and bottom surfaces of the detectors, where the charge dead layer may otherwise compromise the detector discrimination capability.

The capability of the detectors to distinguish photon backgrounds from WIMP-induced nuclear recoils is demonstrated using photon and neutron calibration sources; the neutrons serve as test particles to induce nuclear-recoil events. In separate calibration runs the detectors are alternately exposed to photons from a ^{60}Co source and neutrons (as well as photons) from a ^{252}Cf source.

Figures 1 and 2 show histograms of the charge yield Y, or the ratio of the charge-mediated energy measurement to the phonon-mediated energy measurement, for NTD and QET detectors, respectively. These data show that 99% of photon-induced recoils are rejected while high acceptance is maintained for nuclear recoils. The events between the main recoil peaks are due to electrons that deposit energy in the dead layer and thus have a low charge yield relative to electron recoils in the bulk.

The remainder of the experimental apparatus consists of specialized low-activity detector-housing modules mounted in a shielded cryostat made from a set of nested copper cans. The cans are cooled by conduction through a set of concentric horizontal tubes extending in a dog-leg from a dilution refrigerator. The cryostat is shielded externally with lead, to reduce the flux of photons, and polyethylene, to reduce the flux of neutrons [12]. Samples of all materials internal to the shield are carefully screened in a low-background HPGe counting facility for radio contaminants. Further shielding close to the detectors is achieved with ancient ultra-low-activity lead which has a low concentration of ^{210}Pb, a beta-emitter. Due to the complexity of the detectors and cryostat the first phase of the experiment is being performed at a shallow site at Stanford University at a depth of 17 meters water-equivalent (mwe). Since the cosmic-ray muon flux is reduced by only a factor of 5 at this depth, further rejection of backgrounds is achieved with a hermetic plastic-scintillator muon veto.

3 Results

3.1 Data Sets

Several data runs have been taken in the low-background facility over the past two years, indicating that the experiment can successfully operate over months-long timescales with energy resolutions comparable to those for calibration data. The rates of photon and neutron backgrounds have been consistent with or less than the expected levels, confirming that our goals at the shallow site are attainable and that our screening procedures are effective in limiting these sources of background.

The rate versus energy from a 1.60 kg-d exposure of a 165-g NTD-based germanium detector shows a number of features (Figure 3). The uppermost curve is the full data set (following event quality cuts) and is dominated by photon events coincident with the muon veto; the peak at 9 keV is due to florescence of copper by muon-related photons. The middle curve, events in anti-coincidence with the muon veto, represents a factor of 20 reduction in rate. The line at 10 keV is consistent with internal ^{68}Ge, which undergoes electron capture and leads to a ^{68}Ga x-ray. The broad distribution below 18 keV is due to electrons from tritium decay on the surface of the detector. We have also observed a tritium distribution in events intrinsic to the NTD-Ge thermistors and have since demonstrated that tritium diffuses out of the NTDs at 550 C, similar to the temperature used during the eutectic bonding. It should therefore be possible to control this contamination in future detectors by baking the NTD prior to bonding.

A cut on charge yield to select nuclear recoils, which is based on a fit to neutron calibration data, results in the solid histogram in Figure 3. At low energy, the spectrum is dominated by the tritium events that have low charge yield and survive the cut. Above the tritium endpoint the remaining events are likely due primarily to beta emitters in surface contaminants such as ^{40}K from human perspiration or ^{210}Pb from radon plating. Further steps are now being taken to control the contamination by a surface etch of the detectors late in the fabrication process and through more careful handling following the final etch (e.g., storage in dry nitrogen or vacuum). We also expect to reduce our susceptibility to beta sources external to the detectors by self-shielding them in a close-packed geometry. Finally, work is continuing on reducing the dead layer so that surface-electron events are distinct from nuclear-recoil events; current results appear promising.

The energy resolution of the QET-based detector quoted above is due to a recent 10-fold increase in phonon collection. Prior to this improvement, an exposure of 0.52 kg-d was obtained with a previous 100-g silicon detector. Figure 4 shows rate versus energy for these data. As with the germanium data, the muon veto reduces the rate by a factor of 20. The number of events in the nuclear-recoil region above the threshold of 30 keV are consistent with the expected number of misidentified photons.

3.2 Preliminary Dark Matter Limits

The rates of events consistent with nuclear recoils from the two data sets described above yield upper limits (calculated following reference [7]) on the WIMP-nucleon cross section for spin-independent couplings. Figure 5 shows these limits versus WIMP mass along with other experimental bounds [13,14]. Also shown is the region expected for minimal supersymmetric models (MSSM) that give a relic density greater than 10% of the critical density for a Hubble parameter of 50 km/s/Mpc [5]. Although our exposure is far less than those of the previous experiments, the sensitivity is comparable, thus clearly demonstrating the advantage of background discrimination.

4 Current Status and Plans

Earlier runs have revealed that the primary background source presently limiting our sensitivity consists of low-energy electrons that suffer reduced charge collection. For the current data run, the NTD detectors have been re-etched to remove surface contamination. The improved QET detector currently running should indicate the promise of fiducial-volume cuts using timing information. For future runs, improved cleanliness procedures, increased detector self-shielding, and improved charge collection technologies all should help minimize the surface-electron background and restore the full effectiveness of our event discrimination technique. Once this has been accomplished, we expect to be limited by the cosmogenic neutron backgrounds at the Stanford site with an exposure of about 100-kg-d. To obtain this exposure we will instrument two silicon and four germanium devices with QET readout and six germanium devices with NTD readout, for a total of 200 g of silicon and 2 kg of germanium. Comparison of backgrounds in the Ge and Si will provide information on the backgrounds, especially neutrons. Multiple scattering of neutron backgrounds in the detector arrays will also provide a handle for background subtraction.

In order to take full advantage of these advanced detectors, we plan to continue the experiment at the Soudan Mine. The 2000 mwe overburden at Soudan attenuates cosmic-ray muons by some 5 orders of magnitude, which will greatly reduce cosmogenic activity in the apparatus and greatly reduce the neutron background. Figure 5 shows the expected sensitivity for a 100-kg-d exposure at the Stanford site and a 5000-kg-d exposure at the Soudan site. For reference, the projected sensitivity of the CRESST experiment is also included [15]. As seen in the figure, the CDMS experiments will explore a significant new region of WIMP parameter space, and, in particular, a region where supersymmetric models could provide the dark matter.

Acknowledgment

This work was supported by the Center for Particle Astrophysics, an NSF Science and Technology Center operated by the University of California, Berkeley, under Cooperative Agreement No. AST-91-20005, and by the Department of Energy under contracts DE-AC03-76SF00098, DE-FG03-90ER40569, and DE-FG03-91ER40618.

We gratefully acknowledge the skillful and dedicated efforts of the technical staffs at LBNL, Stanford University, UC Berkeley, and UC Santa Barbara.

References

[1] V. Trimble, Ann. Rev. Astron. Astrophys. **25** (1987) 425 .

[2] E.W. Kolb and M.S. Turner, *The Early Universe* Addison-Wesley, Reading, 1988.

[3] K.A. Olive, astro-ph/9707212.

[4] B.W. Lee and S. Weinberg, Phys. Rev. Lett. **39** (1977) 165 .

[5] G. Jungman, M. Kamionkowski and K. Griest, Phys. Rep. **267** (1996) 195 .

[6] E.I Gates and M.S. Turner, Phys. Rev. Lett. **72** (1994) 2520 .

[7] P.F. Smith and J.D. Lewin, Phys. Rep. **187** (1990) 203 .

[8] Reviewed in N. Booth, B. Cabrera and E. Fiorini, Ann. Rev. Nucl. Part. Sci. **46** (1996) 471 .

[9] CDMS papers can be found at `cfpa.berkeley.edu/group/directdet/gen.html`.

[10] T. Shutt *et al.*, *Proceedings of the 7th International Workshop on Low Temperature Detectors* (Munich, Max Planck Institute of Physics) (LTD7), 224, 1997.

[11] T. Shutt *et al.*, Phys. Rev. Lett. **69** (1992) 3425 ; R.J. Gaitskell *et al.*, LTD7 *ibid.* 221; R.M. Clarke *et al.*, LTD7 *ibid.* 229; A.K. Davies *et al.*, LTD7 *ibid.* 227.

[12] A. Da Silva *et al.*, Nucl. Instrum. Meth. **A354** (1995) 553 .

[13] D.O. Caldwell *et al.*, Phys. Rev. Lett. **65** (1990) 1305 ; M. Beck *et al.*, Phys. Lett. B **336** (1994) 141 ; E. Garcia *et al.*, Phys. Rev. **D51** (1995) 1458 ; A. Morales (private communication).

[14] R. Bernabei *et al.*, Phys. Lett. B **389** (1996) 757 .

[15] M. Buhler *et al.*, Nucl. Instrum. Meth. **A370** (1996) 237 .

Figure captions

Fig. 1. NTD-based germanium detector: charge yield in the recoil-energy range of 15–45 keV for ^{60}Co data (black) and ^{252}Cf data (grey). Photon rejection of 99% is obtained for a nuclear-recoil acceptance of 98%.

Fig. 2. QET-based silicon detector: charge yield in the recoil-energy range of 10–30 keV for ^{252}Cf data. Photon rejection of 99% is obtained for a nuclear-recoil acceptance of 95%.

Fig. 3. Event rate versus recoil energy for a 1.60 kg-d exposure of a 165-g NTD-based germanium detector. The shaded histogram comprises events that pass the nuclear recoil cut.

Fig. 4. Event rate versus recoil energy for a 0.52 kg-d exposure of a 100-g QET-based silicon detector (prior to 10-fold increase in sensitivity).

Fig. 5. The WIMP-nucleon cross section for spin-independent couplings versus WIMP mass. Upper limits on the cross section are shown for earlier runs of CDMS (preliminary), published results using NaI scintillators and Ge diodes, and the goals for CDMS and the CRESST experiment. The shaded region in the lower part of the graph indicates the region where supersymmetric particles could be the dominant dark matter.

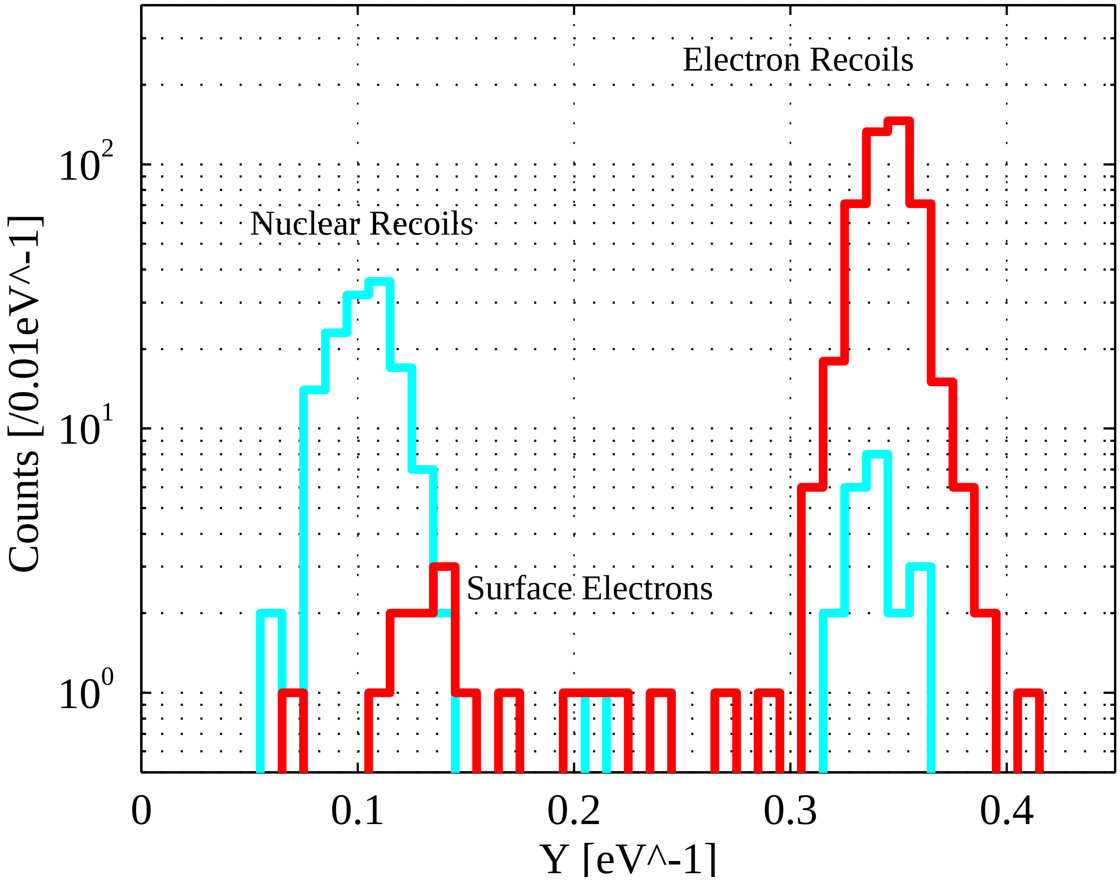
Electron Recoils
Nuclear Recoils
Surface Electrons
Counts [/0.01eV^-1]
10^2
10^1
10^0
0
0.1
0.2
0.3
0.4
Y [eV^-1]

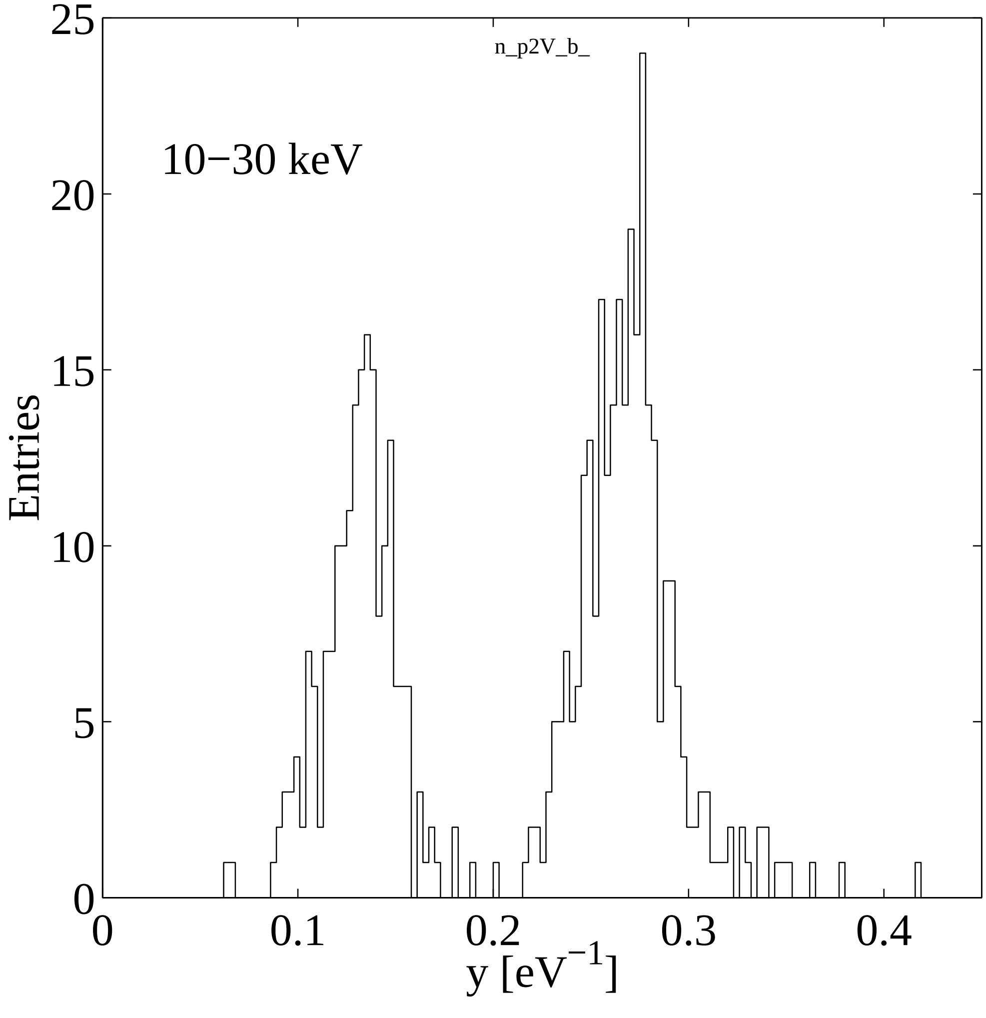
n_p2V_b_
10−30 keV
Entries
y [eV^{-1}]
0
5
10
15
20
25
0
0.1
0.2
0.3
0.4

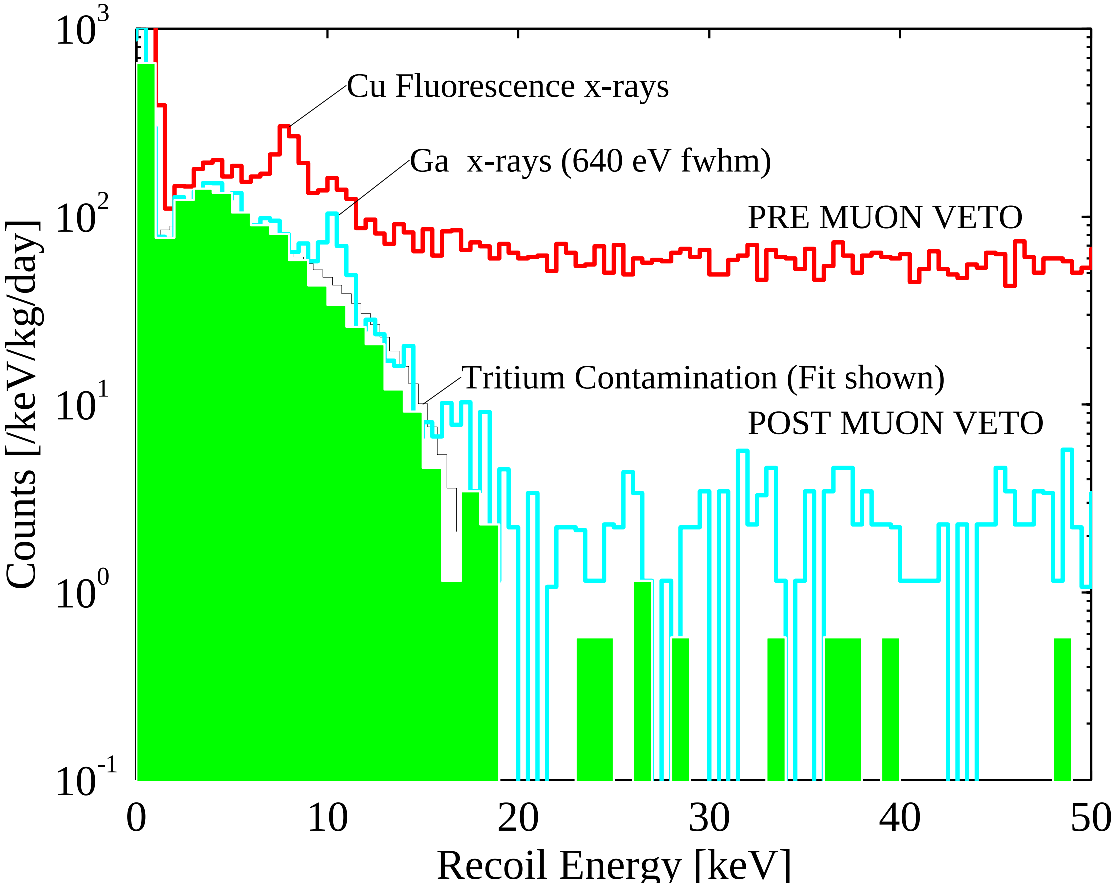

Cu Fluorescence x-rays
Ga x-rays (640 eV fwhm)
PRE MUON VETO
Tritium Contamination (Fit shown)
POST MUON VETO
Counts [/keV/kg/day]
10^3
10^2
10^1
10^0
10^{-1}
0
10
20
30
40
50
Recoil Energy [keV]

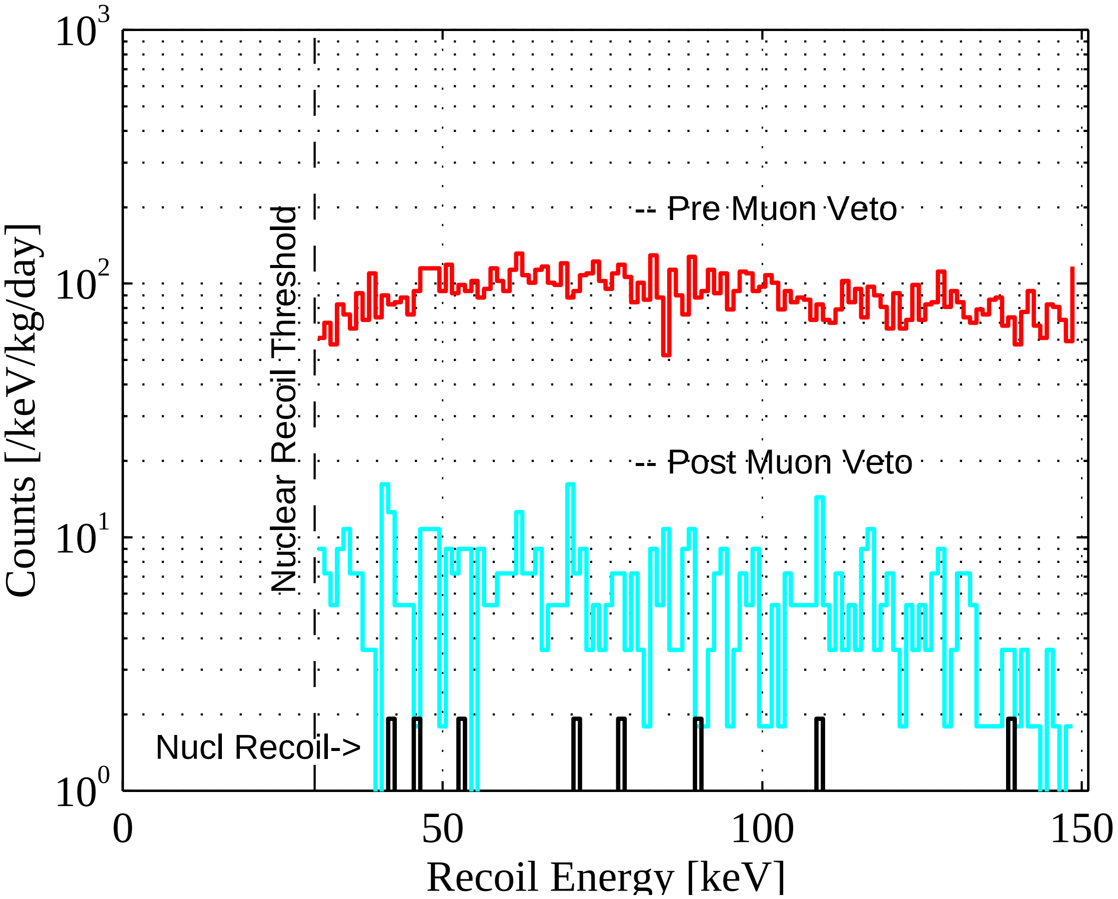

10^3
10^2
10^1
10^0
Counts [/keV/kg/day]
Nuclear Recoil Threshold
-- Pre Muon Veto
-- Post Muon Veto
Nucl Recoil->
0
50
100
150
Recoil Energy [keV]

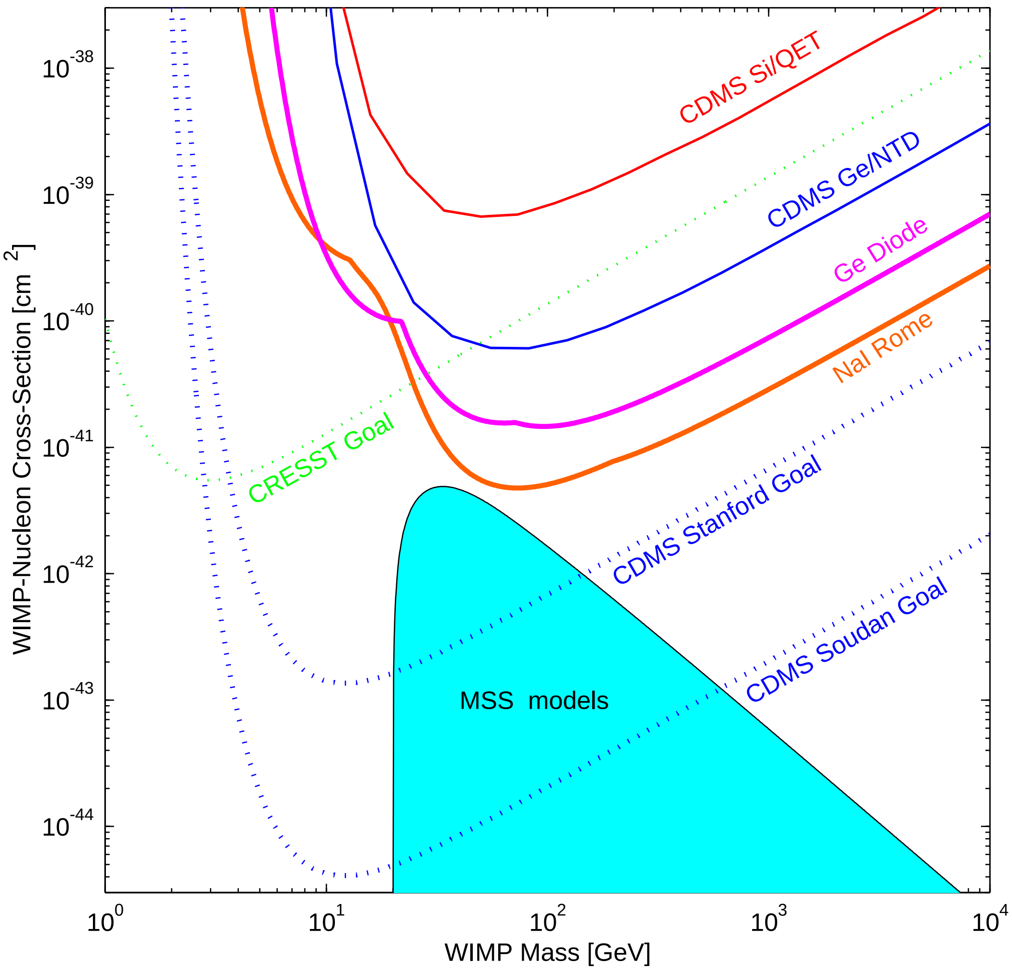

CDMS Si/QET
CDMS Ge/NTD
Ge Diode
NaI Rome
CRESST Goal
CDMS Stanford Goal
CDMS Soudan Goal
MSS models
WIMP-Nucleon Cross-Section [cm ^{2}]
10^{-38}
10^{-39}
10^{-40}
10^{-41}
10^{-42}
10^{-43}
10^{-44}
10^0
10^1
10^2
10^3
10^4
WIMP Mass [GeV]